Petrographic and geochemical characteristics of dolomites in the Devonian Shogram Formation, Karakorum Ranges, North Pakistan

Maryam Saleem[1], Faisal Rehman[2], Abbas Ali Naseem[2,*], Emadullah Khan[3], Syed Wasim Sajjad[2] and Zubair Ahmed[2]

[1]Department of Earth and Environmental Sciences, Bahria University, Islamabad, Pakistan
[2]Department of Earth Sciences, Quaid-i-Azam University Islamabad, Islamabad 45320, Pakistan
[3]Department of Geology, Abdul Wali Khan University, Mardan, Pakistan

Excellent outcrops of Devonian carbonate rocks are present in the Karakorum Ranges of North Pakistan that are highly dolomitized. The Devonian Shogram Formation comprises both matrix and cement dolomite. Petrographic studies revealed the texture of matrix dolomite as fine-grained anhedral dolomite (D1), medium-grained subhedral to anhedral dolomite (D2), medium-grained euhedral dolomite (D3) and coarse-grained anhedral dolomite (D4). The saddle cement dolomite phase of hydrothermal origin precipitated in vugs and fractures. The origin of various dolomitization phases has been interpreted based on petrographic associations, elemental and stable isotopes signatures of each phase. The first two phases of dolomitization are affiliated with the compaction flow of overlying shales based on evidence of low Fe and Mn content and isotopically light signatures of $\delta^{18}O$. The increase in burial resulted in the third phase of dolomite showing signatures of redox conditions and high depleted $\delta^{18}O$ compared to the original marine signatures. The final phases of matrix dolomite and saddle dolomite cement are associated with tectonic activity in the Karakorum region, which brought the deep-source Mg-rich fluids along the Reshun Fault.

Keywords: Dolomites, fractures, petrographic studies, tectonic activity, vugs.

DOLOMITE is a carbonate mineral that forms by dolomitization of limestone[1]. Economic base-metal deposits and hydrocarbon reservoirs formed by hot-fluid circulations are commonly associated with dolomite[2]. About 80% of North America and 50% of the world's carbonate reservoirs occur within dolomite[3]. The dolomitization process destroys partially or completely the original texture of the precursor limestone. In recent years hydrothermal dolomite has gained a lot of attention[4]. It demonstrates a high temperature of formation and is used to evaluate the burial depth[5]. Earlier dolomites were classified based on their texture diversity[6] and later by a modified classification system. Sibley and Gregg[7] presented a classification based on crystal boundary and size distribution. Crystal boundaries will be either planar or non-planar. Planar crystals have many face junctions, whereas non-planar crystal boundaries have curved, serrated, lobate, or irregular face junctions[3]. Planar dolomite had formed due to the faceted crystals growth of early-stage diagenesis, whereas non-planar dolomite had formed due to non-faceted growth of crystals[3]. Dolomites are characterized by planar crystal boundaries developed at below 50°C (ref. 7) while dolomites have non-planar crystal boundaries developed at higher temperatures (above 50°C)[3]. In general, the crystalline shape of mineral is the function of growth kinetics, while crystal order and size depend on its growth and nucleation[3].

Tectonic setting

The present study area is a part of the Karakoram Ranges (Figure 1 *a*), which had tectonically evolved during the Pliocene uplift as a product of the Indian–Asian continental collision[8]. The Karakoram block is located south of the Eurasian plate, with the Pamir Fault to its north and its southern portion thrust over the Kohistan Island Arc. Toward the east and west, it is bounded by Karakoram and Sarobi faults respectively[9]. From south to north, the Karakoram block is divided into three main tectonic units, i.e. the Southern Metamorphic Belt, the Karakoram Batholith and the North Karakoram Terrain. The Southern Metamorphic Belt has undergone pre- and post-collisional metamorphic events, which is evident by the presence of interlayered kyanite or sillimanite-grade pelites, garnet + clinopyroxene amphibolites and dolomitic beds[8]. The Karakoram Batholith is located in the central part of the Karakoram terrane, which encompasses pre-collision.

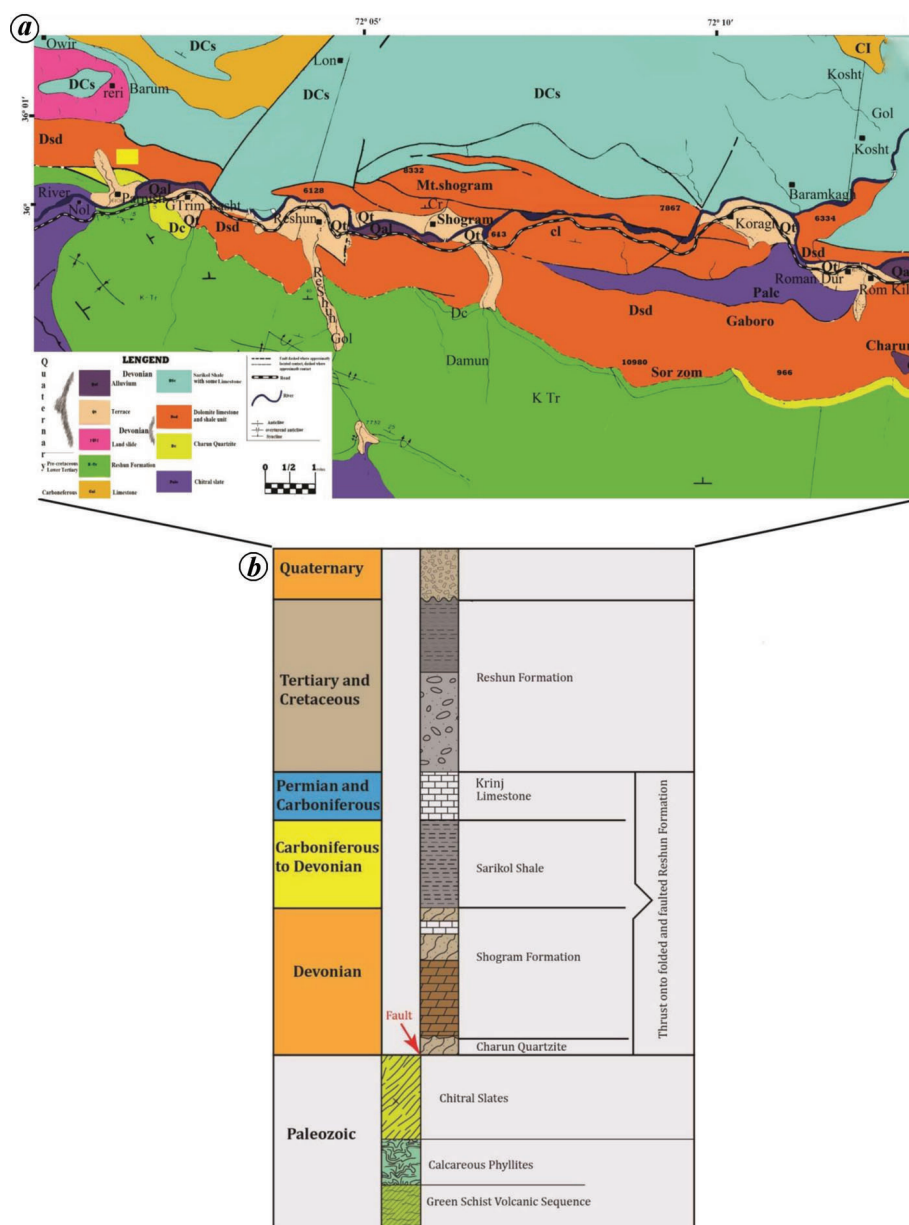*For correspondence. (e-mail: abbasaliqau@gmail.com)

Figure 1. *a*, Geological map of the study area in Chitral, Pakistan. *b*, Stratigraphic column of the study area[33].

Andean-type subduction-related granites and post-collisional crustal melt monzogranites and leucogranites[9]. The North Karakoram Terrain is a belt of sedimentary sequence of the Permian to Cretaceous period and comprises thick and poly-phase stack of thrust sheets[10]. The regional thrust fault of the Karakoram block includes Reshun, Upper Hunza and Chaprusan thrust faults, whereas the Ayun, Naz Bar and Shishi faults contribute to the small-scale thrust fault system[11]. The present study was conducted in Chitral, a part of the westward continuation of their northern sedimentary belt of the Karakoram block (Figure 1 *a*). It is a limited and narrow belt of the Devonian to Triassic rock sequence, as shown in Figure 1 *b* in a simplified stratigraphic column.

Methodology

Field work was carried out in the dolomitized hills and sampled for laboratory studies. A total of 151 samples were collected and cut into slabs, followed by thin-section preparation. Petrographic examinations on thin sections were performed using conventional microscopy at the Department of Earth Sciences, Quaid-i-Azam University Islamabad, Pakistan. The thin sections were previously stained with Alizarin Red-S and potassium ferricyanide to differentiate calcite from dolomite and ferron carbonate from non-ferroan carbonate[12]. To determine major and trace element composition, the inductively coupled plasma-optical emission spectrometry (ICP-OES) technique was
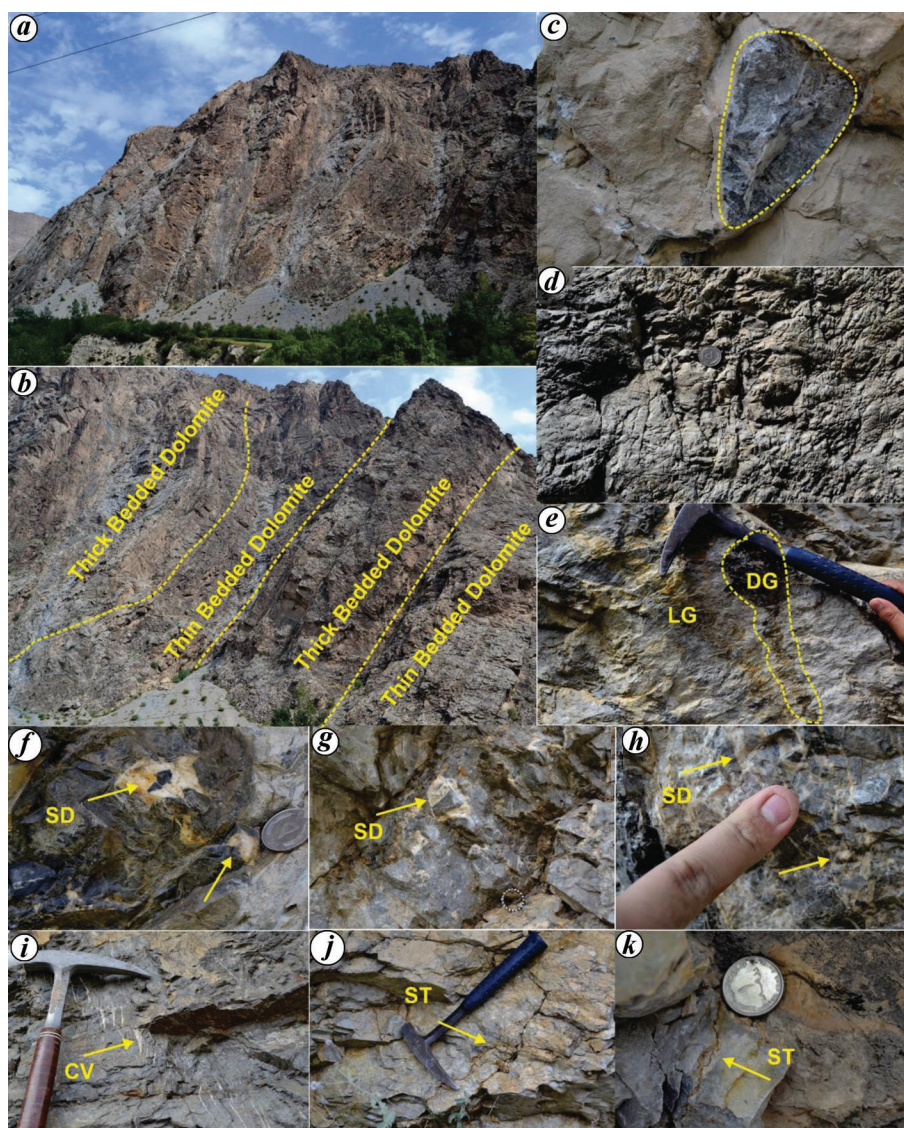
Figure 2. Representative field photographs of Shogram Formation, Parpish section. **a**, **b**, Outcrop view comprising alternating thick- and thin-bedded dolomite. **c**, Dark grey-coloured dolomite on fresh surface. **d**, Chop-board weathering. **e**, Light grey (LG) and dark grey (DG) coloured dolomite. **f**, **g**, Vugs occluded by cementing phase saddle dolomite (SD). **h**, Occurrence of saddle dolomite (SD) in veins and vugs. **i**, Slicken lines filled with calcite. **j**, **k**, Low-angle stylolite (ST) passing through dolomite.

used to evaluate 41 samples at the Pakistan Institute of Nuclear Sciences and Technology (PINSTECH). Eighteen samples were selected from different dolomites for stable oxygen and carbon isotopic study, which were analysed at the Isotope Application Division of PINSTECH. All $\delta^{13}C$ and $\delta^{18}O$ values were expressed per mill (‰) relative to Vienna Pee Dee Belemnite (V-PDB).

Field observations

The studied outcrop of Parpish section comprised of an alternating thick- and thin-bedded, light grey-coloured dolomite (Figure 2 *a* and *b*). The weathered surface of dolomites was light grey, whereas the fresh surface was dark grey (Figure 2 *c*). The diagnostic feature of dolomite, i.e. chop-board weathering, was also observed (Figure 2 *d*). Moreover different types of dolomites were seen cross cutting each other (Figure 2 *e*). Field observations revealed the presence of vugs and fractures, filled with various cementing agents like saddle dolomite, calcite and pyrite minerals. The vugs were mostly irregular in shape with variable size, cemented by the late-stage coarse, crystalline, saddle dolomite SD (Figure 2 *f*). In some places, the occluded vugs were separated from one another by the thin to thick veneer of host dolomite (Figure 2 *g*). SD also enclosed various pores and veins (Figure 2 *h*). Several slicken lines were observed, which were filled with calcite cement (Figure 2 *i*). Low-angle stylolite passed through
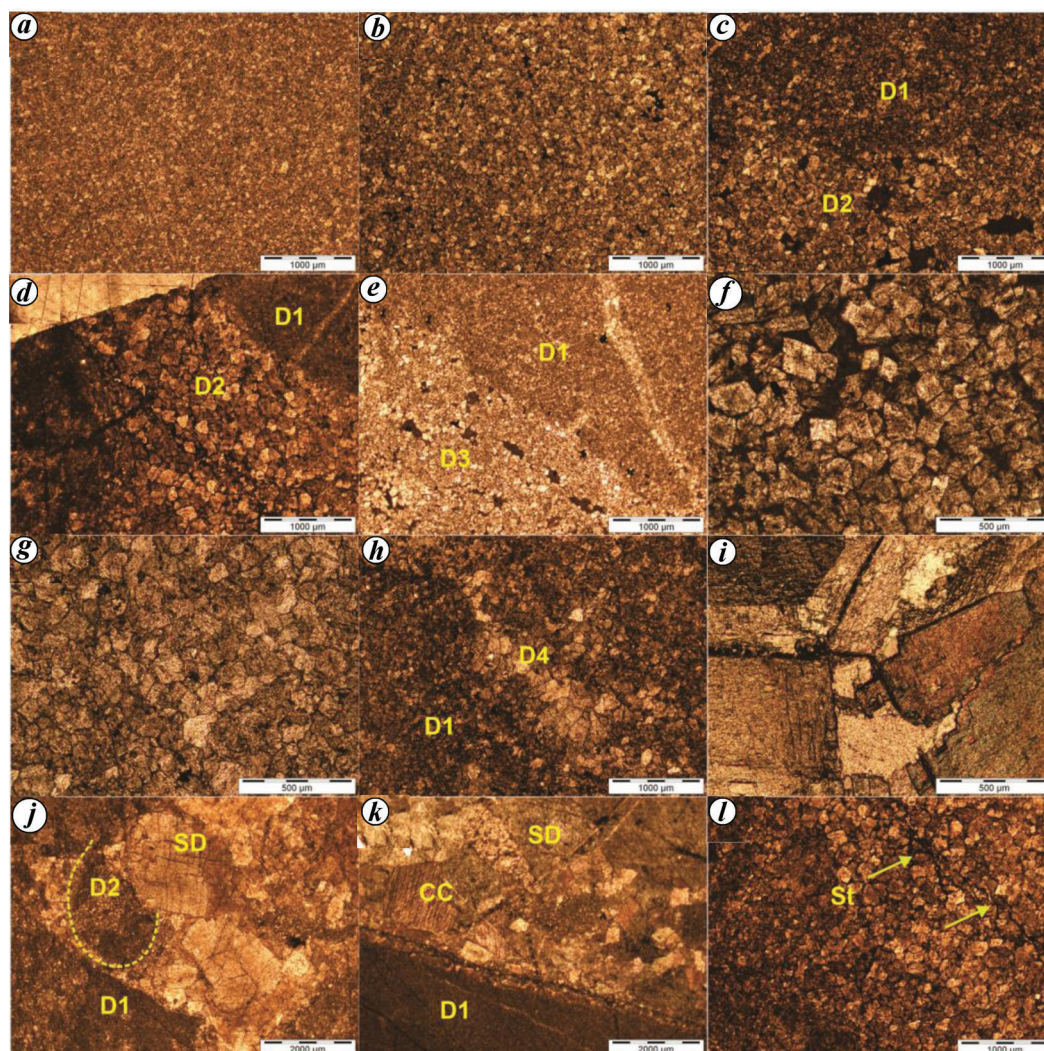
Figure 3. Microscopic examination of different dolomite phases. *a*, Fine-grained anhedral dolomite D1. *b*, Medium-grained subhedral to anhedral dolomite (D2). *c*, *d*, Sharp contact between D1 and D2. *e*, Sharp contact between medium-grained euhedral dolomite D3 and dolomite D1. *f*, Medium grained euhedral dolomite D3. *g*, Coarse-grained anhedral dolomite (D4). *h*, Dolomite D4 crosscut early phase dolomite D1. *i*, Coarse crystalline cementing phase saddle dolomite (SD). *j*, Dolomite D1 with dolomite D2 and cementing phase saddle dolomite SD. *k*, Occurrence of calcite cementation (CC) and saddle dolomite (SD) in contact with fine-grained anhedral dolomite D1. *l*, Late-stage stylolite (St) crosscutting the early phase dolomite D2.

the dolomite rock body, which was infilled by rusty yellow pyrites (Figure 2 *j* and *k*).

Petrography

In petrography, two different dolomite phases were recognized, namely matrix dolomite and cementing dolomite phases. The dolomites display interlocked, euhedral, subhedral to anhedral crystal rhombic morphology, where intercrystalline porosity was diminished. Using the classification of Sibley and Gregg[7], four replacive matrix dolomite phases were distinguished: (i) fine-grained anhedral dolomite (D1); (ii) medium-grained subhedral to anhedral dolomite (D2); (iii) medium-grained euhedral dolomite (D3), and (iv) coarse-grained anhedral dolomite (D4).

D1 exhibited nonplanar, anhedral crystal rhombs with crystal sizes ranging from 20 to 40 µm (Figure 3 *a*). It obscured the original texture of the precursor limestone. The crystal size of dolomite D2 ranged from 80 to 230 µm having nonplanar, subhedral to anhedral, rhombic crystal morphology (Figure 3 *b*). A sharp contact between D1 and D2 was also observed (Figure 3 *c*), where at some places D2 crosscut D1 (Figure 3 *d*). The crystal of D3 ranged from 200 to 300 µm and showed a sharp contact with dolomite D1, cross-cutting the dolomite (Figure 3 *e* and *f*). The anhedral and coarsely crystalline dolomite D4 was the last phase of dolomitization. The crystal size of D4 ranged from 200 to 620 µm (Figure 3 *g*), and D4 crosscut the earlier formed, fine-grain dolomite D1 (Figure 3 *h*). SD represents the coarse-grained cementing phase
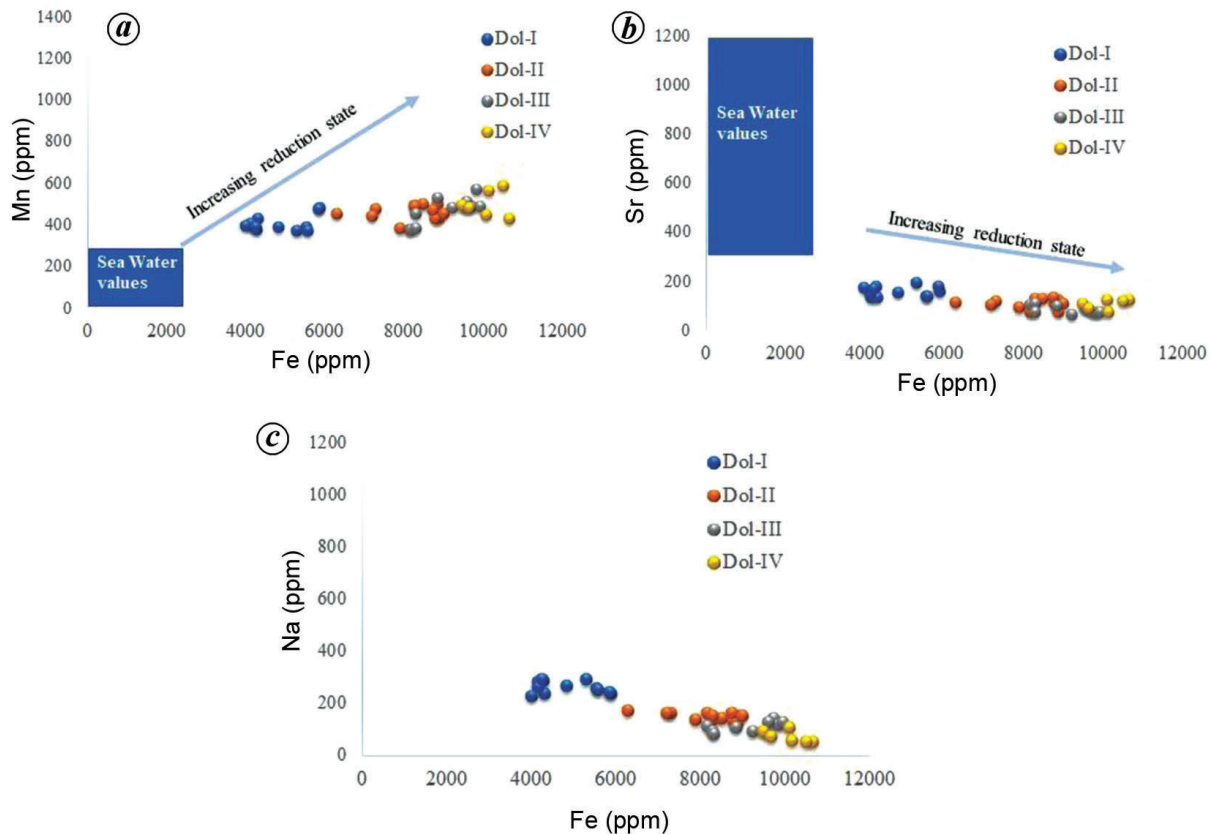
Figure 4. Cross plots of major and trace element concentration. *a*, Enrichment of Fe and Mn showing increase in reduction state in dolomites compared to seawater values. *b*, Concentration of Sr and Fe in different dolomites. The Sr content decreases compared to seawater values. *c*, Concentration of Na and Fe in different dolomite phases.

of dolomitization with sizes ranging from 400 µm to 1 mm (Figure 3 *i*). SD occurred in contact with D1 and D2 (Figure 3 *j*). Fracture and pore-filling calcite cementation was observed (Figure 3 *k*). Stylolite also occurred, which crosscut the earlier formed dolomite D2 (Figure 3 *l*).

Geochemistry

Inductively coupled plasma-optical emission spectroscopy

The major and trace elements in dolomite provide valuable information about the diagenetic process, dolomite origin, diagenetic solution and the mechanisms of dolomitization[13,14]. To determine the chemical composition of dolomites, ICP-OES analyses were carried out (Figure 4). Dolomite D1 comprised of Fe, 4027–5972 ppm; Mn, 372–479 ppm; Sr, 131–188 ppm and Na, 231–195 ppm. D2 had Fe, 6402–8957 ppm; Mn, 372–492 ppm; Sr, 76–131 ppm, and Na, 115–169 ppm. Dolomite D3 had Fe, 8189–9979 ppm; Mn, 376–548 ppm, Sr, 71–105 ppm, and Na, 84–135 ppm, whereas D4 had Fe, 9580–10,564 ppm; Mn, 425–584 ppm; Sr, 78–120 ppm, and Na, 43–101 ppm.

Oxygen and carbon isotope analysis

Representative samples were selected for $\delta^{18}O$ and $\delta^{13}C$ isotope analysis based on the identified phases of dolomite from petrographic results. The correlation of $\delta^{18}O$ and $\delta^{13}C$ values were carried out with the original Devonian seawater signatures. The known oxygen isotope signatures of Devonian seawater for host limestone prior to interaction with magnesium-rich fluids ranged from –3.8‰ to 4.2‰ V-PDB and those of carbon ranged from 0‰ to 1.9‰ V-PDB, while the Devonian marine dolomite $\delta^{13}C$ ranged from 0.5‰ to 2.5‰ V-PDB and those of $\delta^{18}O$ ranged from –2.5‰ to –0.5‰ V-PDB (ref. 15). Figure 5 shows the oxygen and carbon composition of various diagenetic phases of dolomite from the Shogram Formation. These diagenetic phases revealed a wide range of isotopic signatures. D1 showed $\delta^{18}O$ signatures ranging from –6.72‰ to –6.1‰ V-PDB, whereas the $\delta^{13}C$ signatures ranged from 1.2‰ to 1.9‰ V-PDB.

D2 showed depleted isotopic signatures compared to D1 (Figure 5). The $\delta^{18}O$ values of D3 were highly depleted, ranging from −9.1‰ to –8.8‰ V-PDB, whereas the $\delta^{13}C$ values ranged from 0.9‰ to 1.4‰ V-PDB. The matrix dolomite D4 showed highly depleted isotopes signatures,
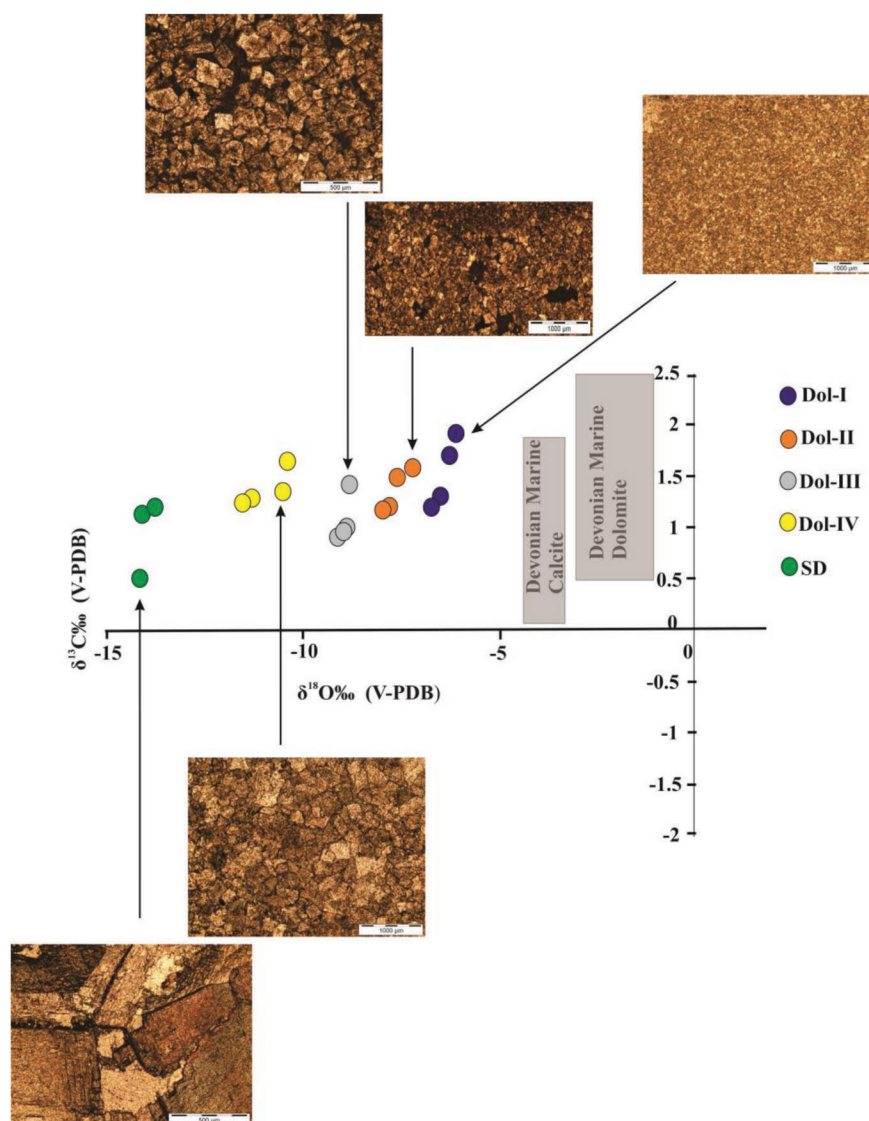
Figure 5. Oxygen and carbon isotope signatures of various dolomite phases compared to middle Devonian marine limestone and dolomite indicated by grey box[34].

and their $\delta^{18}O$ and $\delta^{13}C$ values ranged from $-11.5‰$ to $-10.4‰$ V-PDB and $1.2‰$ to $1.6‰$ V-PDB respectively. The saddle dolomite (SD) exhibited the highest depleted $\delta^{18}O$ values ranging from $-14.1‰$ to $-12.4‰$ V-PDB, whereas $\delta^{13}C$ values were within the range of the original marine signatures, i.e. $0.51–1.4‰$ V-PDB.

Discussion

The study area has experienced various stages of deformation. During the Late Permian to Early Triassic, rifting of Karakorum block from Gondwanaland followed by compressional tectonism of the Late Cretaceous due to Kohistan–Karakorum collision resulted in widespread plutonism[15]. Four stages of deformation occurred in the Karakorum block after the Kohistan–Karakorum colli-

sion[16]. The Paleocene to Eocene deformations were related to granitic magmatic intrusions, metamorphism and crustal thickening, followed by the Indian–Eurasian collision during the Eocene. The southward motion along the Main Karakorum Thrust (MKT) was active since the closure of the Indus Suture, and up to Miocene and thereafter. The Dextral motion was also observed along the MKT associated with reverse faulting[16].

In the study area, the Reshun Fault has thrusted Devonian Shogram Formation over the Cretaceous Reshun Formation (Figure 2 a)[17]. A detailed paragenetic sequence has been established based on field observations, petrographic study, and geochemical analysis of the studied outcrop of the Shogram Formation, which revealed a multistage diagenetic evolution (Figure 6). These multistage dolomitization events in the Devonian Shogram
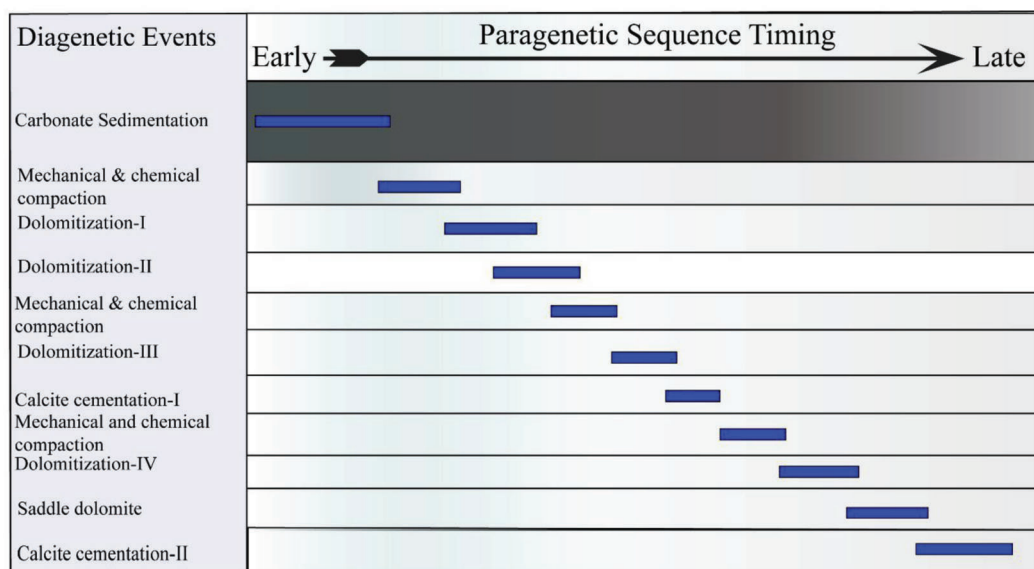
Figure 6. Various digenetic events of dolomite and calcite phases that occurred over time.

Formation are discussed below. The D1 had partially inherited the original nature of limestone, where the peloidal structure of the host limestone has been replaced (Figure 3 *c*). D2 exhibited a coarser crystal rhomb, but showed similarity in texture to D1. Coarsening in dolomite crystal size occurs due to factors like precipitation rate, increased temperature and overgrowth of later-stage dolomites on existing cores of earlier dolomites[18]. D3 showed cloudy centres and clear rims (Figure 3 *f*). The cloudy centre often indicates post-depositional replacive dolomitization[19]. This dolomite was formed either from direct carbonate replacement or through recrystallization of early dolomite types D1 and D2 (ref. 21). D4 showed undulose extinction and distorted crystal lattice, which indicate crystal growth at high temperatures (>60°C) during deep burial settings[20]. The occurrence of cementing phase saddle dolomite revealed the most profound diagenetic settings for their formation during progressive burial, which followed replacive matrix phases and occluded the brittle fracturing. Calcite cementation occurred after the activation and reactivation of faults at different times, which caused intense fracturing in dolomite (Figure 3 *k*). The diagenetic process in dolomite is controlled by the dolomitizing fluids, which can be traced through different elemental concentrations like sodium, strontium, manganese and iron[13]. Previous studies showed that during carbonate diagenesis, Mn concentration increases and Sr decreases[21]. The studied dolomite phases showed a significant amount of Mn (Figure 4 *a*) and a low concentrations of Sr (Figure 4 *b*), which are comparable to dolomites precipitated from marine waters[22]. Sr content >300 ppm has been predicted for dolomites formed from normal marine seawater[23]. This is significantly more Sr than that contained in the Devonian Shogram Formation.

The Sr concentration exhibited an inverse relation with crystal size and showed a significant decrease with increasing crystal size[24]. Unlike Sr, Fe and Mn concentrations showed a reducing state environment for diagenetic and dolomitizing fluids. Dolomite D3 and D4 showed higher concentrations of Fe and Mn compared to D1 and D2, suggesting their formation under reducing conditions during burial diagenesis[25]. The distribution of Fe and Mn in solution is strictly controlled by redox conditions and their concentrations in precursor limestone and precipitation rate[13].

Stable isotope analyses of dolomites showed a pronounced shift of δ^{18}O values from the original Devonian marine signatures of calcite and dolomite (Figure 5). The non-depleted δ^{18}O signatures revealed their formation in the surface environment of evaporitic condition[26]. Stable isotope values showed a wide range of δ^{18}O values, mainly between −11.98‰ and −5.153‰ V-PDB, which is reliable with multiphase diagenetic history[27,28]. Dolomite D1 represents the first of the replacive dolomite phase and shows less depleted δ^{18}O signatures from D2, which suggests a relatively low temperature for its formation compared to D2. In the case of D3, δ^{18}O signatures are more depleted with reference to D1 and D2, suggesting its formation from the buffering of host limestone at a higher temperature from the preceding dolomite phases. The measured δ^{18}O values showed further depletion from the original marine Devonian signatures and a most pronounced shift was observed in D4 (Figure 5). Dolomite D4 formed at a much higher temperature than the early diagenetic dolomite phases. The latter phases reveal heavier δ^{18}O values and are formed at a lower temperature compared to the later diagenetic dolomites with lighter δ^{18}O values[29]. Similarly, vugs and veins filling the

cementing phase saddle dolomite showed high depletion of δ^{18}O values (Figure 5). The more pronounced negative shift of oxygen isotopic trend of saddle dolomite (–14.53‰ to –11.98‰ V-PDB) suggests high-temperature fluid from a greater depth than the replacive dolomitizing fluids. This late-stage saddle dolomite indicates higher temperatures[30]. All the observed diagenetic phases showed a shift towards negative oxygen isotope signatures, and increased temperature is the likely source of depleted δ^{18}O values.

Mechanism of dolomitization

As discussed earlier, the Devonian Shogram Formation has undergone various episodes of deformation and plutonism. Based on stratigraphic and structural settings, field observations, petrographic studies and geochemical analysis, the burial dolomitization model has been suggested for the studied outcrop of the Shogram Formation (Figure 7). In general, burial dolomitization models are essentially hydrological models which differ in terms of the drives and direction of fluid flow[31]. The development of non-planar crystal textures at more than 60°C and the presence of saddle dolomite suggest a temperature of more than 80°C. The initial phases of dolomitization (D1 and D2) resulted from the compactional dewatering of the overlying Sarikol Shales, where the fractures acted as a conduit to the underlying Shogram Formation, causing the initial dolomitization, which is supported by the low Fe and Mn contents and less depleted δ^{18}O values. Increasing burial

Figure 7. Dolomitization model for the Devonian Shogram Formation where dolomitization occurred in two stages.

resulted in the formation of D3, which is evident by additional redox conditions at depth and high depleted values of δ^{18}O. Finally, activation of the regional Reshun Fault provided pathways for Mg-rich dolomitizing fluids from the deeper source resulting in the formation of D4 and saddle dolomite, as evident by the more depleted δ^{18}O values and the presence of certain hydrothermal minerals, like willemite and merwinite. Other high-temperature minerals like kutnohorite and bustamite were also associated with D4 (ref. 32). The source of Mg-rich hydrothermal fluid in D4 could be the widespread igneous intrusion in the Karakorum region during collisional or post-collisional periods.

Conclusion

The Devonian Shogram Formation in the northwestern Karakorum was examined in detail through field observations, petrographic studies and geochemical analysis. In the petrographic studies, four replacive matrix dolomite types and cementing saddle dolomite phases were recognized. The influence of diagenetic and hydrothermal fluids was traced through Fe and Mn concentrations. All dolomite phases showed high Fe and Mn contents; these were very high in dolomite D3 and D4, which suggests an environment of reducing conditions. The variation of Sr concentration in different dolomite phases suggests a multistage diagenetic process. D1 had the lowest and D4 had the highest Sr content, indicating a later diagenetic environment for D4 compared to D1. The oxygen–carbon isotope signatures suggest that all the studied dolomites have been formed under variable temperature conditions. The measured δ^{18}O V-PDB values of fine-grained dolomites were higher than those of D2, D3 and D4. This less-depleted δ^{18}O values of D1 suggest lower formation temperature. D3 and D4 have more depleted δ^{18}O values, indicating multiphase dolomitization and high-temperature origin. Furthermore, saddle dolomite cement exhibited highly depleted δ^{18}O values, indicating a very high temperatures. The conceptual dolomitization model suggests three phases of dolomitization events. Initially, replacive dolomites (D1 and D2) were formed by compactional dewatering of the overlying shale to cause dolomitization in shallow burial conditions, which is supported by petrographic and geochemical data. This was followed by deep burial conditions, which resulted in the formation of dolomite D3, evident by highly depleted δ^{18}O values and enhanced Fe and Mn contents. D4 and SD are associated with the activation of the NE–SW Reshun Fault, which has provided pathways for the Mg-rich hydrothermal fluids, supported by highly depleted δ^{18}O values, high Fe and Mn contents and the presence of high-temperature hydrothermal minerals along with dolomite D4, which is evident from the recrystallization and formation of coarse crystals in D4. The coarse crystal size in association with an increase in burial conditions, lower concentration of
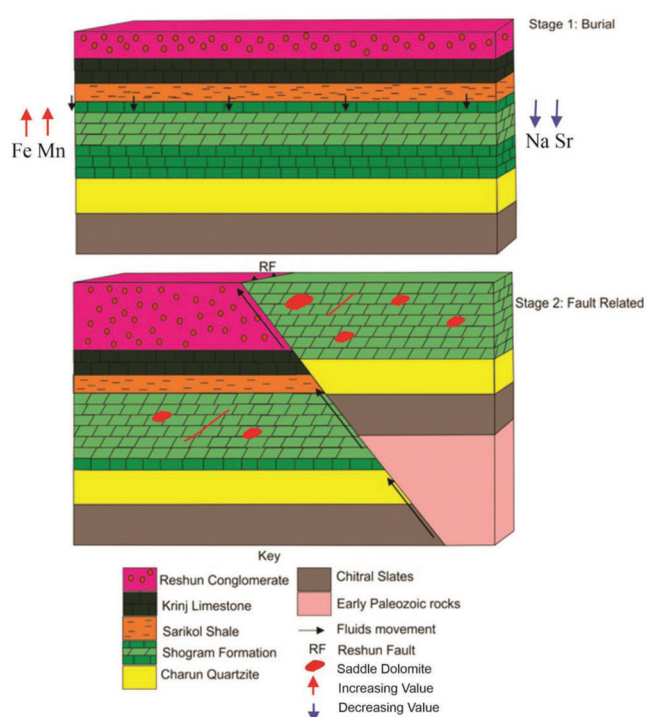
Na, Sr, higher amounts of Mn and Fe, and the depleted oxygen isotope values indicate that replacive dolomites of the Shogram Formation are recrystallized by diagenetic solutions at increased temperature during burial. The possible source of hydrothermal fluids in later stages could be magmatic or deep-seated, which circulated along the faults.

1. Peyravi, M., Rahimpour-Bonab, H., Nader, F. H. and Kamali, M. R., Dolomitization and burial history of lower triassic carbonate reservoir-rocks in the Persian Gulf (Salman offshore field). *Carbonates Evaporites*, 2008, **30**, 25–43.
2. Navarro-Ciurana, D., Corbella, M., Cardellach, E., Vindel, E., Gómez-Gras, D. and Griera, A., Petrography and geochemistry of fault-controlled hydrothermal dolomites in the Riópar area (Prebetic Zone, SE Spain). *Mar. Pet. Geol.*, 2016, **71**, 310–328.
3. Warren, J., Dolomite: occurrence, evolution and economically important associations. *Earth Sci. Rev.*, 2000, **52**, 1–81.
4. Davies, G. R. and Smith, L. B., Structurally controlled hydrothermal dolomite reservoir facies: an overview. *AAPG Bull.*, 2006, **90**, 1641–1690.
5. Machel, H. G., Concepts and models of dolomitization: a critical reappraisal. *Geol. Soc., London, Spec. Publ.*, 2006, **235**, 7–63.
6. Friedman, G. M., Terminology of crystallization textures and fabrics in sedimentary rocks. *J. Sediment. Res.*, 1965, **35**, 643–655.
7. Sibley, D. F. and Gregg, J. M., Classification of dolomite rock textures. *J. Sediment. Res.*, 1987, **57**, 967–975.
8. Lemennicier, Y., Le Fort, P., Lombardo, B., Pêcher, A. and Rolfo, F., Tectonometamorphic evolution of the central Karakorum (Baltistan, northern Pakistan). *Tectonophysics*, 1996, **260**, 119–143.
9. Searle, M. P., Geological evolution of the Karakoram Ranges. *Ital. J. Geosci.*, 2011, **130**, 147–159.
10. Le Fort, P. and Gaetani, M., Introduction to the geological map of the western Central Karakorum, North Pakistan. Hindu Raj, Ghamubar and Darkot regions. 1 : 250,000. *Geologica*, 1998, **3**, 3–57.
11. Calkins, J. A., Jamiluddin, S., Bhuyan, K. and Hussain, A., Geology and mineral resources of the Chitral-Partsan area, Hindu Kush Range, northern Pakistan (No. 80-837). US Govt. Print. Off.; for sale by the Distribution Branch, US Geological Service, 1980.
12. Dickson, J. A. D., Carbonate identification and genesis as revealed by staining. *J. Sediment. Res.*, 1966, **36**, 491–505.
13. Veizer, J., Chemical diagenesis of carbonates: theory and application of trace element technique. *J. Sediment. Res.*, 1983, 265–300.
14. Humphrey, J. D. and Quinn, T. M., Coastal mixing zone dolomite, forward modeling, and massive dolomitization of platform-margin carbonates. *J. Sediment. Res.*, 1989, **59**, 438–454.
15. Gaetani, M., The Karakorum block in central Asia, from Ordovician to Cretaceous. *Sediment. Geol.*, 1997, **109**, 339–359.
16. Zanchi, A., Gaetani, M. and Poli, S., The rich gol metamorphic complex: evidence of separation between Hindu Kush and Karakorum (Pakistan). *CR Acad. Sci.*, *Ser II*, 1997, **325**, 877–882.
17. Dawans, J. M. and Swart, P. K., Textural and geochemical alternations in late Cenozoic Bahamian dolomites. *Sedimentology*, 1988, **35**, 385–403.
18. Hou, M. C., Jiang, W. J., Xing, F. C., Xu, S. L., Liu, X. C. and Xiao, C., Origin of dolomites in the Cambrian (upper 3rd-Furongian) formation, south-eastern Sichuan Basin, China. *Geofluids*, 1993, **16**, 856–876.
19. Machel, H. G., Concepts and models of dolomitization: a critical reappraisal. *Geol. Soc. London, Spec. Publ.*, 2004, **235**, 7–63.
20. Huang, S. J., Shi, H. and Mao, X. D., Diagenetic alteration of earlier Palaeozoic marine carbonate and preservation for the information of sea water. *J. Chengdu Univ. Technol.*, 2003, **30**, 9–18.
21. Machel, H. G. and Anderson, J. H., Pervasive subsurface dolomitization of the Nisku Formation in central Alberta. *J. Sediment. Res.*, 1989, **59**, 891–911.
22. Banner, J. L., Hanson, G. N. and Meyers, W. J., Water–rock interaction history of regionally extensive dolomites of the Burlington-Keokuk Formation (Mississippian): isotopic evidence. In *Sedimentology and Geochemistry of Dolostones* (eds Shukla, V. and Baker, P. A.), 1988.
23. Swart, P. K., The geochemistry of carbonate diagenesis: the past, present and future. *Sedimentology*, 2015, **62**(5), 1233–1304.
24. Zheng, X., Arps, P. J. and Smith, R. W., Adsorption of *Bacillus subtilis* to minerals: effect on the flotation of dolomite and apatite. *Process Metall.*, 1999, **9**, 127–136.
25. Lorens, R. B., Sr, Cd, Mn and Co distribution coefficients in calcite as a function of calcite precipitation rate. *Geochim. Cosmochim. Acta*, 1981, **45**, 553–561.
26. Montañez, I. P. and Read, J. F., Eustatic control on early dolomitization of cyclic peritidal carbonates: evidence from the Early Ordovician Upper Knox Group, Appalachians. *Geol. Soc. Am. Bull.*, 1992, **104**, 872–886.
27. Swart, P. K., Cantrell, D. L., Westphal, H., Handford, C. R. and Kendall, C. G., Origin of dolomite in the Arab-D reservoir from the Ghawar Field, Saudi Arabia: evidence from petrographic and geochemical constraints. *J. Sediment. Res.*, 2005, **75**, 476–491.
28. Swart, P. K., The geochemistry of carbonate diagenesis: the past, present and future. *Sedimentology*, 2015, **62**, 1233–1304.
29. Radke, B. M. and Mathis, R. L., On the formation and occurrence of saddle dolomite. *J. Sediment. Res.*, 1980, **50**, 1149–1168.
30. Morrow, D. W., Diagenesis 2. Dolomite-part 2 dolomitization models and Ancient dolostones. *Geosci. Can.*, 1982, **9**, 95–107.
31. Morrow, D., Regional subsurface dolomitization: models and constraints. *Geosci. Can.*, 1998, **25**.
32. Saleem, M., Dolomitization in Devonian Shogram Formation, Chitral North Pakistan: multiple constraints from field analysis, petrography, geochemistry and diagenetic studies. Doctoral Dissertation, Quaid e Azam University, Pakistan, 2022.
33. Stauffer, K. W., Reconnaissance geology of the central Mastuj valley, Chitral State, Pakistan (No. 75-556), US Geological Survey, Chitral, 1975.
34. Popp, B. N., Anderson, T. F. and Sandberg, P. A., Textural, elemental, and isotopic variations among constituents in Middle Devonian limestones, North America. *J. Sediment. Petrol.*, 1986, **56**, 715–727.